



The Compact Muon Solenoid Experiment

CMS Note

Mailing address: CMS CERN, CH-1211 GENEVA 23, Switzerland



May 30, 2006

CMS ECAL intercalibration using laboratory measurements

F. Cavallari, S. Costantini, I. Dafinei, M. Diemoz, E. Longo, P. Meridiani, G. Organtini, R. Patamatti

Dipartimento di Fisica, Università "La Sapienza" and INFN, Sezione di Roma, Roma, Italy

R. Egeland, M.M. Obertino^{a)}, R. Rusack

University of Minnesota, Minneapolis, Minnesota 55455, USA

E. Auffray, P. Lecoq, P. Sempere-Roldan

CERN, Geneva, Switzerland

N. Pastore

Dipartimento di Fisica, Università di Torino and INFN, Sezione di Torino, Torino, Italy

F. Fetti, G. Franzoni, A. Ghezzi, P. Govoni, M. Paganoni, S. Ragazzi, C. Rovelli, T. Tabatelli

Università degli Studi "Milano Bicocca" and INFN, Sezione di Milano, Milano, Italy

Abstract

The CMS electromagnetic calorimeter is presently under construction at CERN. Inter-calibration of the channels is a crucial issue for physics performance. The main source of channel-to-channel response variation in the barrel is the crystal-to-crystal variation of scintillation light yield which has an RMS of 8%. An improved method of using laboratory measurements performed during the ECAL assembly phase to provide an initial intercalibration is presented. The intercalibration constants derived from these measurements are compared to reference coefficients measured using high energy electrons in a test-beam. It is found that the intercalibration coefficients obtained from the laboratory measurements have an RMS precision of about 4%.

^{a)} now at Università di Torino and INFN Sez. di Torino, Italy.

1 Introduction

Establishing an inter-calibration of the CMS ECAL crystal calorimeter channels to be used at start-up of the LHC collider operations is important for setting initial trigger threshold, to guarantee a reasonable energy resolution and to ensure a sufficiently uniform response of the calorimeter. For the barrel ECAL, only a few of the 36 supermodules, each made of 1700 crystals, will be exposed to high energy electron test beam for inter-calibration studies. Laboratory measurements, performed in the construction phase, can be used to derive intercalibration coefficients for the remaining channels [2].

The accuracy of an inter-calibration based on laboratory measurements has been verified by comparison with electron test beam data in 2002 [2]. It was shown that the method using knowledge on the light yield and longitudinal transmission of the PbWO_4 crystals, the geometry of the crystals, and the associated photo-sensitive and amplification electronics, can be used to achieve a precision of 4.5%. This precision was seen to critically depend on the determination of the light yield of the crystals.

In this paper, a comparison is made with electron test beam data taken in 2003 and an improvement of the inter-calibration method based on laboratory measurements is presented.

1.1 The CMS electromagnetic calorimeter

The CMS Electromagnetic calorimeter [1] is made of about 75000 lead tungstate (PbWO_4) scintillating crystals. It is composed of a barrel and two endcaps. The crystals in the barrel are grouped in 36 supermodules, each divided in 4 modules as shown in Figure 1. The crystal shape varies with η ; in particular there are 17 different types of crystals and for each of them there is a right and left handed version.

The PbWO_4 was chosen because it is fast and has a short radiation length and a small Moliere radius. Nevertheless, its intrinsic light yield is relatively low, about 100 photons/MeV at 18°C. This fact along with the presence of a very intense magnetic field inside the barrel led to the choice of avalanche photodiodes (APDs) as photodetectors. Two APDs, coupled in a capsule, are glued on the rear face of each crystal; five capsules are read out by the same Very-Front-End (VFE) board. The VFEs are connected, in groups of five, to the Front-End (FE) boards, the cards designed to process and store the digitized data while waiting for the trigger decision. The data are transferred to the off detector electronics via optical fibres.



Figure 1: Supermodule of ECAL calorimeter.

Due to the tight construction schedule only a few of the 36 super-modules will be calibrated in a test-beam with high energy electrons before installation in CMS. However, having a starting point for the calorimeter calibration is important for setting the trigger threshold and to guarantee a reasonable initial energy resolution. For the barrel ECAL the main source of channel-to-channel response variation in the barrel is the crystal-to-crystal variation of scintillation light yield which has an RMS of 8%. For those channels that will not be calibrated with the beam, it has been suggested to use the crystal light yield measurements performed in the construction phase. The accuracy of this method can be verified comparing test-beam crystal calibrations with the prediction from laboratory. In the 2002 it was shown that this method can achieve a precision of 4.5% for a large statistics of crystals [2].

This analysis shows that an improvement of this precision can be reached combining all available laboratory

measurements.

1.2 Test beam setup

During Summer 2003 100 crystals of a type 4 module were tested at Cern on the H4 beam of the CERN SPS. The APDs were read out by VFE cards equipped with FPPA (described in [3]) to amplify the signal. The final HV system conceived for the CMS-ECAL was used to supply the APDs. The crate was connected to the module via a cable of 120 m, as it will be for the final installation in the experiment. The module was sitting on a moving Table, which allowed a position scan with the beam. It was cooled and maintained at $18 \pm 0.05^\circ C$.

2 Optical characterization of the $PbWO_4$ crystals

All ECAL crystals are characterized in two regional Centres: CERN and Roma (INFN-ENEA at Casaccia) before assembly. The crystal characterization consists of the measurement of the longitudinal (LT) and transversal (TT) optical transmission, the scintillation light yield (LY) and the dimensions. These measurements are performed in an automatic way with special machines called ACCOS (Automatic Crystal Control System) [4]. The CERN centre has built three ACCOS machines (named ACCOS, ACCOCE1 and ACCOCE2). The Rome centre has 1 machine (ACCOR). Cross calibration of the CERN and Rome machines is described in [5].

The results of Rome measurements have been presented in [6]. The LY and the Longitudinal Transmission (LT) measurements performed at the CERN centre are described in the following sections 2.1 and 2.2.

2.1 Light Yield measurement

At the CERN centre, the LY is measured with the photon counting technique described in Ref. [7]. The measurement involves a scan with a radioactive source in steps of 1 cm along the full crystal length, making use of a step motor. The $PbWO_4$ light is collected by a photomultiplier (PM).

Crystals are accepted if their LY is greater than 8 photoelectrons per MeV (pe/MeV). This limit is set for crystals wrapped in a Tyvek envelope and coupled to the PM with a special optical grease. Only a subset of crystals is tested in this condition. In the ACCOS machines crystals are not wrapped and there is no optical contact between them and the photomultiplier. A set of coefficients is used to convert the ACCOS measurements in to the aforementioned acceptance conditions; they are determined periodically using the crystals tested on both test setups.

The LY versus position measurements are fitted with two straight lines from 3.5 to 11.5 cm from the crystal front and from 11.5 to 19.5 cm. The slope of these fits in units of radiation lengths (X_0) corresponds to the so-called Front and Rear Non-Uniformity. From the fit results the LY at $8 X_0$ (distance corresponding to the shower-maximum for a 50 GeV electrons) is also deduced. This is what is usually referred to as "the LY" of the crystal.

The FNUF is a crucial parameter for the calorimeter performance, because it contributes to the constant term of the energy resolution. Because of the tapered shape of the crystals, a strong focusing effect takes place and so the crystal light yield profile is not naturally flat. In order to have a uniform light yield, one of the lateral faces of the crystals is depolished by the producer. This procedure is discussed in [7]. The crystals for which the FNUF is found outside the specifications are further depolished at CERN. In what follows we will call these crystals "hand-uniformized".

2.2 Longitudinal Transmission Measurement

At CERN the longitudinal transmission (LT) is measured using special spectrophotometers [7]. The light going through the crystal is emitted by a halogen lamp and detected by a large UV-extended pin photodiode. The longitudinal transmission is measured at 11 wavelengths selected with a set of optical filters: 330, 340, 350, 360, 380, 392, 405, 420, 450, 500, 620, 700 nm. A typical LT curve is shown in Figure 2.

It has a plateau for high wavelengths and a steep descent around 360 nm. The LT curve is fitted in the region of the edge with the following function:

$$LT(\lambda) = (1 - P3 \cdot e^{-\lambda/P4}) \cdot e^{-e^{-(\lambda-P0) \cdot P1} \cdot P2} \quad (1)$$

where P4 is fixed to 92 nm. This function has an inflection point on the edge; the slope at the inflection point and the LT at 360 nm are considered as indicators for radiation hardness. The LT at 420 nm and 620 nm are considered for general crystal quality. Crystals are accepted if: $LT(360 \text{ nm}) > 25\%$, $LT(420 \text{ nm}) > 55\%$, $LT(620 \text{ nm}) > 65\%$ and $Slope > 3\%/nm$. In order to improve the precision we use the fit results to determine the LT at 360 nm (LT_{360}).

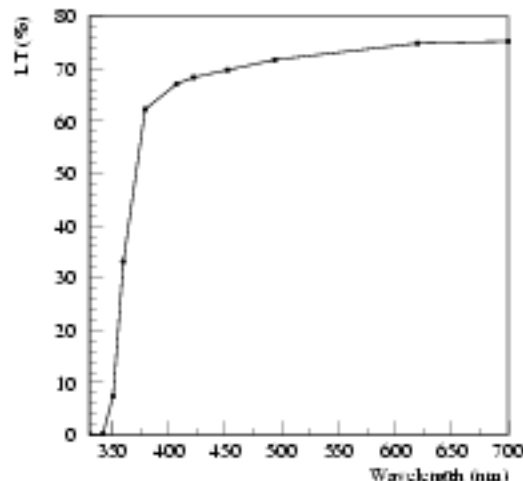


Figure 2: Typical longitudinal transmission curve measured at Cern.

3 Improvement of the Light Yield resolution

Due to the small amount of PbWO_4 scintillation light, it is very difficult to measure precisely the Light Yield for PbWO_4 crystals in the laboratory with low energy radioactive sources. The measurement precision can be improved by applying corrections derived from regular repeated measurements of reference crystals, and also by using the correlation between the measured longitudinal transmittance and the light yield.

3.1 Reference Crystal Correction

A set of reference crystals is measured daily on ACCOS in order to monitor the machine stability [7]. The resolution of the LY measurements can be improved [6] by rescaling each raw crystal LY measurement by the daily measurement of the reference crystals according to the formula:

$$LY_{corr}(\text{crystal } X, \text{day } d) = LY_{raw}(\text{crystal } X, \text{day } d) \cdot \frac{LY_{raw}(\text{crystal Ref}, \text{day } 0)}{LY_{raw}(\text{crystal Ref}, \text{day } d)} \quad (2)$$

Figure 3 shows the measurements of the reference crystal light yield performed by the two CERN ACCOS machines.

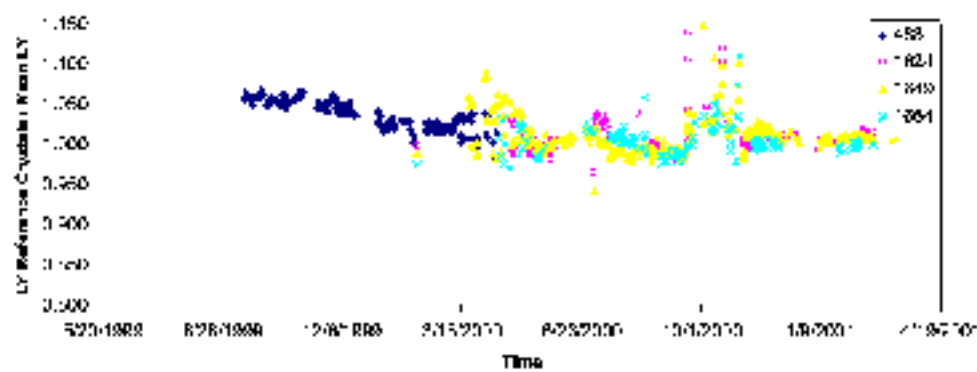
Figures 4 and 5 show the effect of the correction of Eq. (2) on the resolution of the reference crystals. The plots represent the raw and corrected light yield normalized to the value at day 0. The corrected distributions have a resolution which ranges between 0.9% and 1.7%. These results are not as good as the one reported in [6] for ACCOR because at Cern the number of measured reference crystals varies every day while in Rome the same five reference crystals are measured daily. Nevertheless, the improvement clearly visible for the ACCOCE2 crystals confirms the fact that this correction is important in case of large fluctuations of the ACCOS devices. Figure 6 shows all reference crystal measurements in one plot without and with the daily correction. The overall corrected distribution has a standard deviation of about 1.7%. Because of the effectiveness of this correction, in this analysis we use it in the determination of the LY.

3.2 Correlation between longitudinal transmission and light yield.

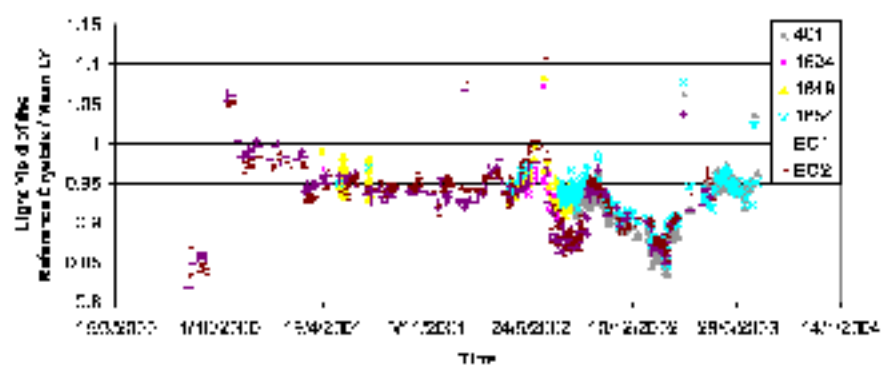
The LT measurement is simpler and more precise than the LY measurement. A correlation of the LT measured at 360 nm and the crystal LY was reported in Ref. [8]. It is proposed here to exploit this correlation between LT_{360} and the LY to improve the precision of the determination of the LY.

The dependence between the LY and the LT_{360} can be fitted by a straight line

$$LY = p_1 + p_2 \cdot LT_{360} \quad (3)$$

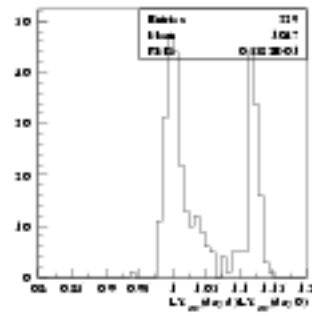


(a)

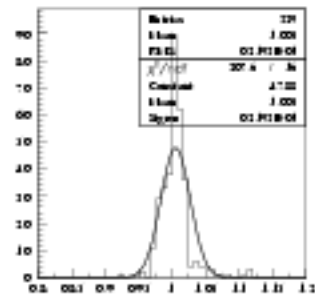


(b)

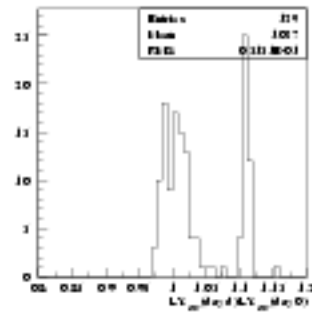
Figure 3: Light yield of the ACCOS (a) and ACCOCE2 (b) reference crystals normalized to their mean light yield as a function of the time.



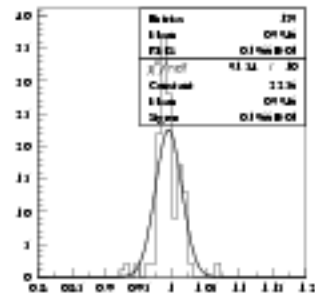
(a)



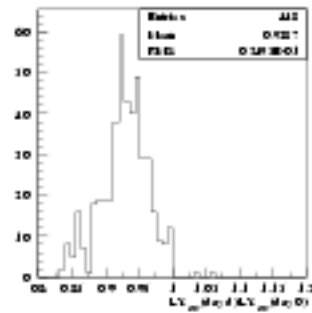
(b)



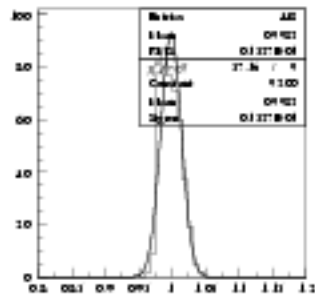
(c)



(d)

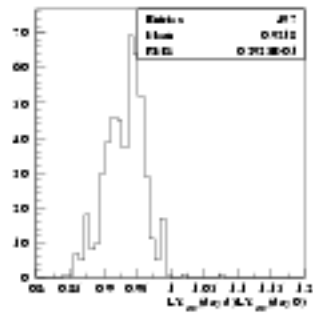


(e)

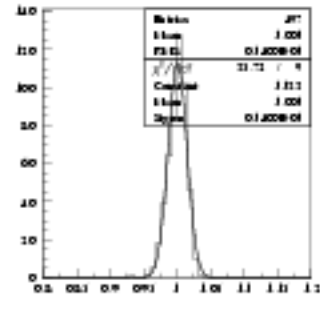


(f)

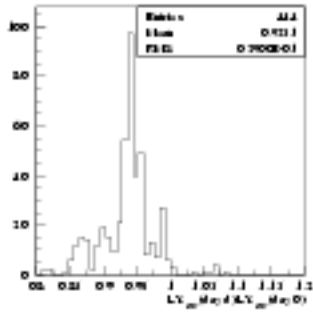
Figure 4: Raw (left plots) and corrected (right plots) light yield for some of the reference crystals measured by ACCOS.



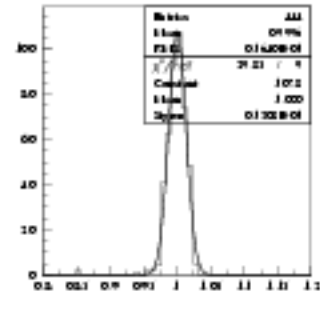
(a)



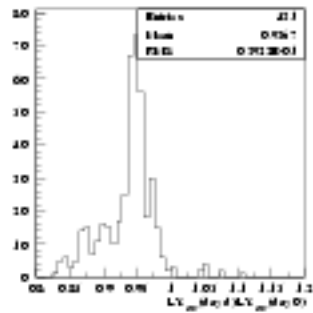
(b)



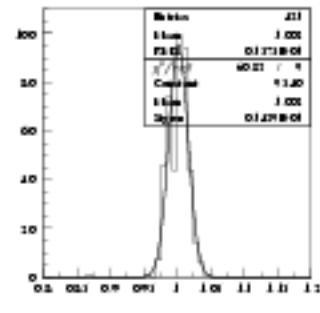
(c)



(d)



(e)



(f)

Figure 5: Raw (left plots) and corrected (right plots) light yield for some of the reference crystals measured by ACCOGE2.

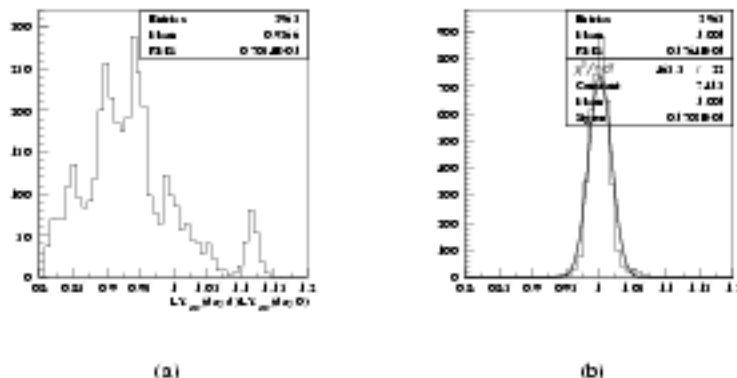


Figure 6: Raw (left plot) and corrected (right plot) light yield for all the reference crystals measured by all ACCOS machines. Every crystal measurement is corrected with the daily measurements of the other reference crystals.

and the parameters $p1$ and $p2$ can be used to derive a new value for the light yield ($LY_{from LT}$).

The crystals measured at Cern so far do not have exactly the same characteristics: the first 4 crystal batches have a single dopant, while from middle of batch 5 onwards the crystals have a double doping. Moreover, the toughness of the depolished face was changed during the pre-production period in order to optimize the FNUF. In this respect, we can distinguish four crystal groups as in Table 1.

Group	Doping	Roughness (μm)	Crystal Type	Batch
0	single	0.25	all	1-5
1	double	0.25	all	5-7
2	double	0.35	all	8-14, P1-P6, S1
3	double	0.30	1	from S2 and from P7
3	double	0.35	2-9	from S2 and from P7
3	double	0.30	10-13	from S2 and from P7
3	double	0.25	14-17	from S2 and from P7

Table 1: Roughness and doping of crystals measured at CERN. The production batches are indicated with letter P and S depending on the contract.

It has been shown in Ref. [7] that the toughness has an effect on the measured LY. Moreover, the measured LY might depend on the crystal type, because of the different shape; so, for the determination of the parameters $p1$ and $p2$ in formula 3, it is appropriate to analyze separately crystals with different toughness and shape. Figure 7 shows the dependence of the LY on the LT_{380} for different kind of crystals.

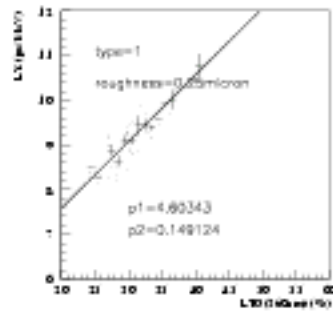
A collection of measurements from the ACCOS and ACCOCE2 machines have been analysed for about 10000 crystals of different batches which were mounted in ECAL supermodules from 0 to 8. The crystals which had been "hand uniformized" have been excluded from this analysis because of their peculiarity. Table 2 shows the parameters $p1$ and $p2$ from the fit of the different groups. In the last column of this Table we also report the calculated LY at $LT_{380}=30\%$. This parameter is independent of the crystal quality of the batch and can be used to compare old and new batches. Figure 8 shows the LY at $LT_{380}=30\%$ versus crystal type for different toughness.

4 Comparison with the test beam data.

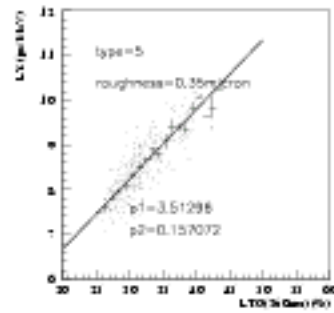
The light yield can be determined using high energy electron beams as

$$LY = \frac{S}{\epsilon_{cont} E_{beam} G_{APD} G_{el} e} \quad (4)$$

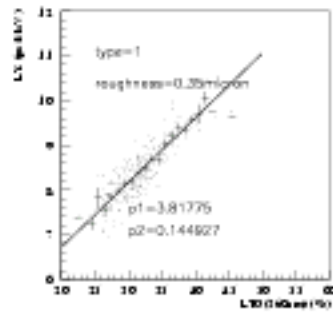
where S is the signal amplitude measured in the central crystal, ϵ_{cont} the containment factor, E_{beam} is the energy of the beam, G_{APD} is the gain of the capsules, G_{el} is the gain of the electronics and e the electron charge.



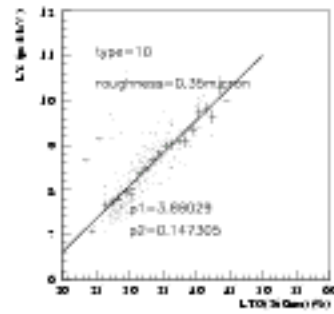
(a)



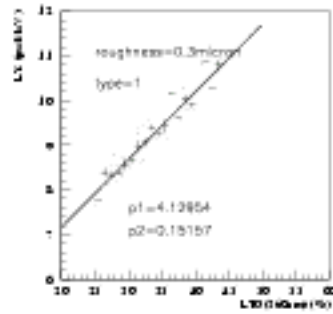
(b)



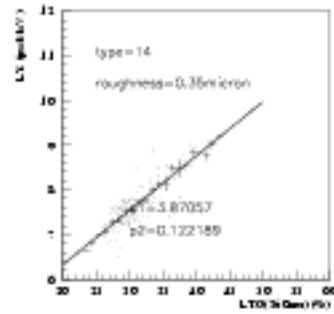
(c)



(d)



(e)



(f)

Figure 7: Light yield versus LT_{360} for different kind of crystals. Plot a,c,e show the dependence on the roughness; plots b,d,f show the dependence on the crystal type.

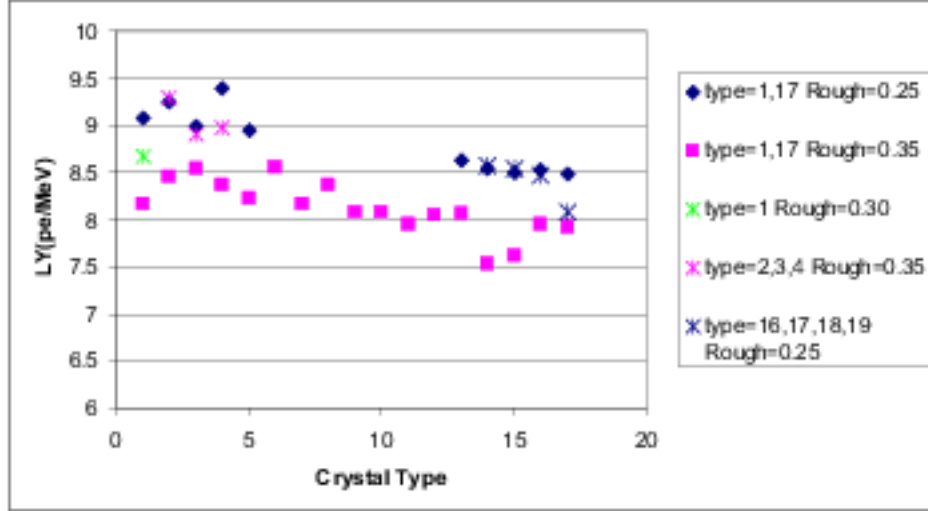


Figure 8: Light yield at $LT_{380}=30\%$ versus crystal type for different roughness.

To compare the measurements performed in the laboratory with the ones performed on beam we have used the method described in [2]. As proposed in this note, we use the relative light yield (RLY), defined as the light yield coefficient of each crystal, normalized to the average:

$$RLY_{Lab(TB)} = \frac{LY_{Lab(TB)}}{LY_{Lab(TB)}^{avg}} \quad (5)$$

and the difference:

$$\Delta RLY = \frac{RLY_{Lab} - RLY_{TB}}{RLY_{Lab}}, \quad (6)$$

In Figure 9 we show the distribution of ΔRLY for the 58 SMO not hand-uniformized crystals calibrated with 120 GeV electron beam. In plot (a) the ΔRLY has been calculated with the raw LY_{Lab} neglecting the APD and the electronics correction in formula 4. A gaussian fit is superimposed to the data. The standard deviation of the distribution is $(4.8 \pm 0.2)\%$ in good agreement with what has been reported for MO' in [2]. We have afterwards applied all corrections proposed in Section 4. Plot (b) represents the distribution obtained correcting for the variation of the reference crystal light yield (formula 2). The standard deviation from the fit is in this case slightly better ($4.6 \pm 0.2\%$) although we do not expect a very big improvement since the crystals mounted on the same module are generally tested in a short period of time. This correction will be more important when we determine the inter-calibration coefficients for crystals of different modules. Figure 9 (c) shows the ΔRLY^i where LY_{Lab} is calculated from LT_{380} as in formula 3. The gaussian fit gives a $\sigma=(4.3 \pm 0.2)\%$. This value compares well with the resolution of plot (b) obtained directly from the light yield measurement. Since the two measurements are independent we have defined the mean light yield as:

$$MEANLY = \frac{LY_{Lab} + LY_{from LT}}{2}. \quad (7)$$

Plot 9 (d) shows the ΔRLY obtained with the MEANLY. The standard deviation of this distribution is $\sigma=(4.1 \pm 0.2)\%$. The improvement of the resolution obtained with the MEANLY method is particularly interesting for the strategy

of initial calibration of the calorimeter. The fact that the MEAN LY is in a better agreement with the test beam light yield suggests that it could give a better prediction of the inter-calibration factor for the supermodule that will not be calibrated with the beam.

Finally we have corrected the data with the real gain of the APDs and of the preamplifier of the VFE board. The results are shown in Fig. 9(e) and 9(f) respectively. The resolution obtained is $\sigma = (4.1 \pm 0.1)\%$. A further correction could come from the ADC calibration which were not available for this module. Figure 10 compares the laboratory and the test beam LY before and after the described corrections.

5 Fine correction for the inter-calibration.

In order to deduce start-up crystal inter-calibrations from the laboratory measurement with the best possible resolution all fine effects should be taken into account. Among these, so far, two effects have been investigated: the variation of the containment factor (ϵ_{cont} in Eq.(4)) and of measured light yield with the crystal type.

5.1 Containment factor

Since crystals have 17 different shapes, in principle the containment factor could vary from type to type. This effect has been investigated using a full Monte Carlo simulation of the test beam described in [9]. Electrons with an energy of 120 GeV were directed at the crystals at reference locations corresponding to the points of maximum containment for 50 GeV electrons (for more details, see [9]). Figure 11 shows the energy contained in a matrix of 1x1, 3x3 and 5x5 crystals versus crystal type. For all crystal types, except the anomalously shaped type 1, the containment varies by less than 0.1%. Even for crystals of type 1 the correction only amounts to 0.5%.

5.2 Dependence of the light yield on the crystal area.

Figure 12 shows the variation of the test crystal area. Crystals of type 1 have a peculiar shape; for the others the area decreases of about 10% from type 2 to 17. The same trend is observed for the light yield in Figure 8. Since the photodetectors used to measure the light yield in the laboratory cover the whole test crystal surface, this is expected. However, the APDs cover a fixed area of the crystal test surface, and it is expected that a correction will need to be applied to the laboratory measurement to account for this difference. Detailed study with ray tracing Monte Carlo might help in understanding the behaviour. Results from the study of a complete supermodule tested in the beam will be available soon.

Conclusion

The laboratory measurements of about 10000 crystals have been analyzed. The reference crystal correction brings an improvement of the light yield resolution important when comparing crystals measured on different machines and at very different times. With this correction the light yield resolution is about 1-1.5%. The correlation between the LT and the LY improves the crystal inter-calibration from laboratory measurements, showing that a resolution of 4% can be obtained. In order to deduce start-up inter-calibration of the crystals from the laboratory measurement with the maximum possible resolution various effects, including fine corrections depending on the crystal geometry, should be taken into account. A comparison of inter-calibration coefficients from laboratory measurements with electron test beam measurements of a full supermodule is required to better masterize all systematic effects.

Acknowledgements

The authors would like to thank the pretious collaboration of the technicians of the Rome/INFN-Casaccia and CERN Lab. 27 Regional Centres. We would also like to thank Yves Sisois for useful comments on this note.

References

- [1] *CMS, the Electromagnetic Calorimeter Project, Technical Design Report, CERN/LHCC 97-33 CMS TDR 4, 15 december 1997.*
- [2] F. Cavallari et al., *Relative Light Yield comparison between laboratory and testbeam data for CMS ECAL PbWO₄ crystals.*, CMS RN 2004/002.

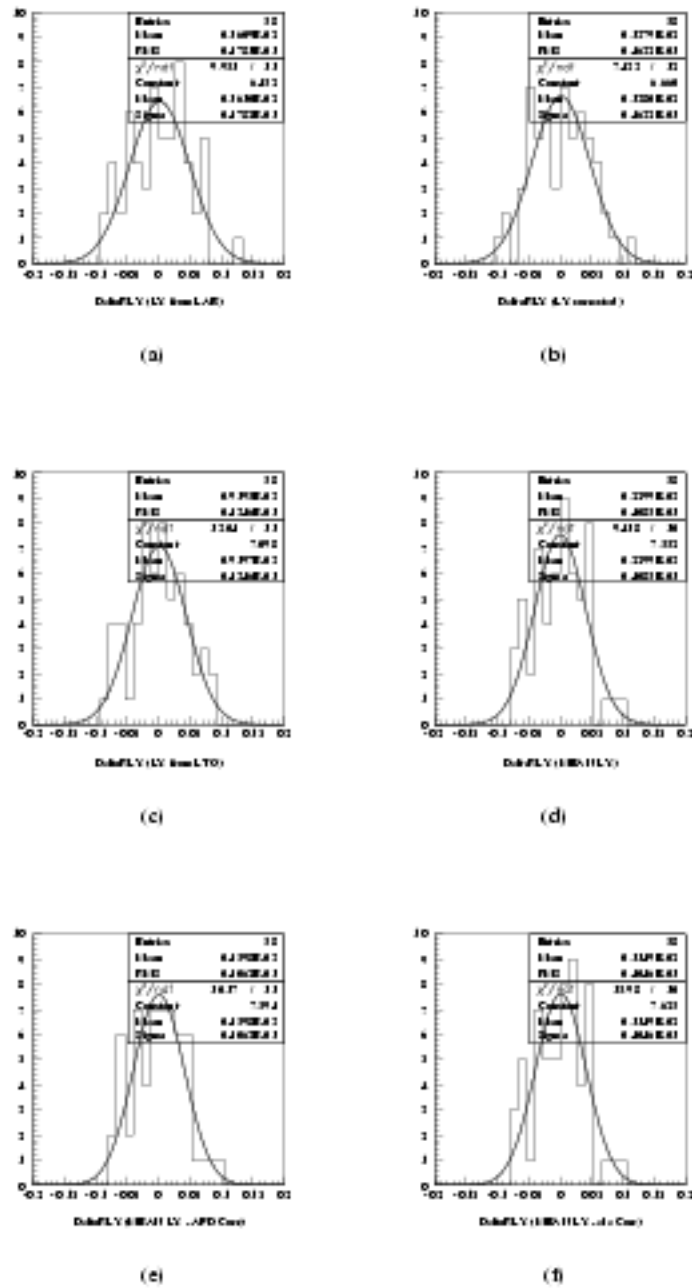


Figure 9: Distribution of ΔRLY for the 58 SMO crystals calibrated with the beam. The different plots show the effect of all corrections described in the text.

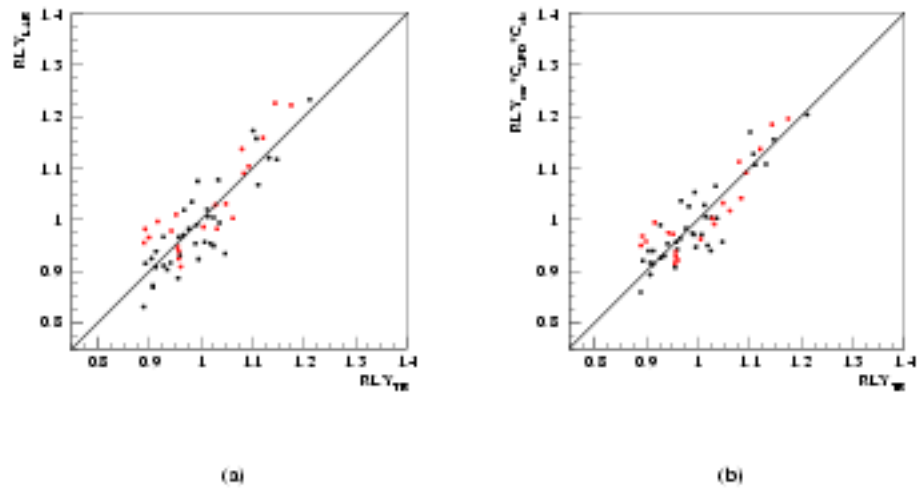


Figure 10: Comparison between the laboratory and the test beam LY before and after the corrections described in the text.

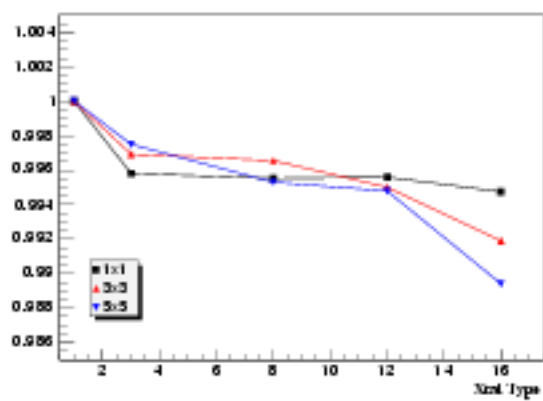


Figure 11: Energy contained in a matrix of 1x1, 3x3 and 5x5 crystals versus crystal type.

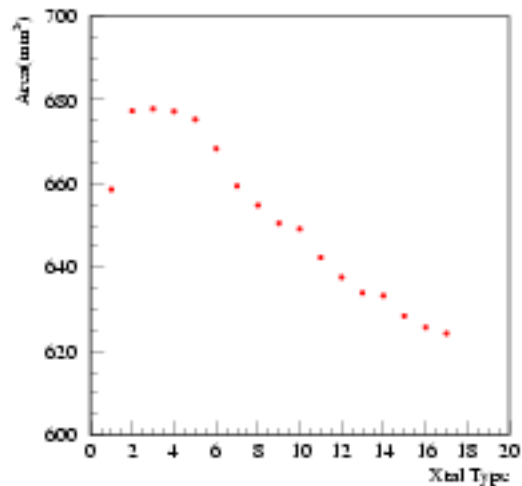


Figure 12: Dependence of the test crystal area on the crystal type.

- [3] J.P. Walker et al., *Custom integrated Front-End circuit for the CMS Electromagnetic Calorimeter*, IEEE Transactions on nuclear science, vol. 48, No.6, Dec. 2001.
- [4] E. Auffray, et al., *Performance of ACCOS, an automatic crystal quality control system for PWO*, CMS NOTE 1999/067
S. Baccaro et al., NIM A 459 (2001) 278-284.
- [5] E. Auffray et al., *Cross-Calibration of Two Automatic Quality Control Systems for the CMS ECAL Crystals*, CMS NOTE 2003/003.
- [6] L. M. Batone et al., *Improvement on PbWO₄ Crystal Inter-calibration Precision from Light Yield Measurements at the INFN-ENEA Regional Center*, CMS RN 2004/003
- [7] P. Sempere-Roldan, *Quality control and preparation of the PWO crystals for the electromagnetic calorimeter of CMS*, PHD Thesis.
- [8] L. M. Batone et al., *Correlation between the light yield and the longitudinal transmission in PbWO₄ crystals and the impact on the precision of the crystals inter-calibration.*, CMS RN 2004/005.
- [9] P. Meridiani, *Detailed comparison between 2003 CMS ECAL Test-Beam Data and a Geant4 based simulation*, CMS Note in preparation.

Type	Roughness (μm)	Group	p1 (pe/MeV)	p2 (pe/MeV/(%))	LY at $LT_{380}=30\%$ (pe/MeV)
1	0.25	1	4.603	0.149	9.077
2	0.25	1	4.801	0.148	9.252
3	0.25	1	4.002	0.166	8.990
4	0.25	1	6.036	0.111	9.391
5	0.25	1	3.996	0.165	8.946
6	0.25	1	no data	no data	no data
7	0.25	1	no data	no data	no data
8	0.25	1	no data	no data	no data
9	0.25	1	no data	no data	no data
10	0.25	1	no data	no data	no data
11	0.25	1	no data	no data	no data
12	0.25	1	no data	no data	no data
13	0.25	1	4.297	0.144	8.629
14	0.25	1	4.868	0.122	8.543
15	0.25	1	3.348	0.171	8.494
16	0.25	1	3.770	0.158	8.528
17	0.25	1	4.186	0.143	8.481
1	0.35	2	3.817	0.144	8.165
2	0.35	2	3.851	0.153	8.452
3	0.35	2	4.104	0.147	8.535
4	0.35	2	3.688	0.155	8.368
5	0.35	2	3.512	0.157	8.225
6	0.35	2	4.427	0.137	8.557
7	0.35	2	4.323	0.127	8.161
8	0.35	2	3.688	0.156	8.369
9	0.35	2	3.849	0.141	8.084
10	0.35	2	3.660	0.147	8.079
11	0.35	2	2.819	0.171	7.955
12	0.35	2	3.727	0.144	8.057
13	0.35	2	3.134	0.164	8.069
14	0.35	2	3.870	0.122	7.536
15	0.35	2	3.831	0.125	7.611
16	0.35	2	4.007	0.131	7.943
17	0.35	2	3.889	0.134	7.915
1	0.30	3	4.129	0.151	8.676
2	0.35	3	5.987	0.110	9.296
3	0.35	3	4.323	0.152	8.908
4	0.35	3	4.380	0.152	8.968
5	0.35	3	no data	no data	no data
6	0.35	3	no data	no data	no data
7	0.35	3	no data	no data	no data
8	0.35	3	no data	no data	no data
9	0.35	3	no data	no data	no data
10	0.30	3	no data	no data	no data
11	0.30	3	no data	no data	no data
12	0.30	3	no data	no data	no data
13	0.30	3	no data	no data	no data
14	0.25	3	4.561	0.133	8.564
15	0.25	3	4.329	0.140	8.546
16	0.25	3	4.366	0.136	8.467
17	0.25	3	4.756	0.110	8.074

Table 2: Parameters derived from the fit of the LY versus LT_{380} for different kind of crystals.